ACADEMIC PRESS

Available online at www.sciencedirect.com
SCIENCE DIRECT®

Journal of Catalysis 214 (2003) 121–129

JOURNAL OF CATALYSIS

www.elsevier.com/locate/jcat

Simulation of kinetic oscillations in the CO + O_2/Pt reaction on the nm scale

V.P. Zhdanov [a,b,*] and B. Kasemo [a]

[a] *Department of Applied Physics, Chalmers University of Technology, S-412-96 Göteborg, Sweden*
[b] *Boreskov Institute of Catalysis, Russian Academy of Sciences, Novosibirsk 630090, Russia*

Received 11 June 2002; revised 6 August 2002; accepted 3 September 2002

Abstract

Using the Monte Carlo technique, we simulate kinetic oscillations in CO oxidation occurring on nm-sized supported Pt particles via the conventional Langmuir–Hinshelwood mechanism and surface oxide formation and removal. Incorporating cooperative effects into the oxide growth mode, we demonstrate that the oscillations may be accompanied by remarkable segregation between oxide and CO. During oscillations, the maximum CO coverage may be appreciably smaller that that at saturation. These findings are in line with recent transient Fourier transform infrared spectroscopy measurements (Fanson, P.T., Delgass, W.N., Lauterbach, I., J. Catal. 204 (2001) 35) indicating that during oscillations on Pt/SiO_2 the CO coverage is relatively low and the shift of the stretching frequency of linearly bonded CO is nearly negligible.

Keywords: CO oxidation; Oxide model; Island formation; Monte Carlo simulations

1. Introduction

Since the first report by Hugo [1], kinetic oscillations in CO oxidation on nm-sized supported Pt crystallites have been observed in many laboratories (see the review by Schüth et al. [2] and references in [3]). In analogy with the same reaction on poly- and single-crystal Pt samples [2], this phenomenon is usually attributed to the interplay of a rapid bistable catalytic cycle and a relatively slow "side" process ("relatively slow" means that the time scale characterising this process is much longer than that of the catalytic reaction), such as formation of surface oxide or subsurface oxygen (these terms are often used interchangeably), carbon deposition, or adsorbate-induced crystallite restructuring. Among the latter processes, oxide formation is often considered the most likely. To clarify this point, Fanson et al. (FDL) [3] recently performed careful transient Fourier transform infrared spectroscopy (FTIR) measurements during kinetic oscillations at intermediate pressures (1–10 Torr) and temperatures (450–570 K) on a series of silica-gel-supported Pt catalysts of varying dispersion and preparation. Well-developed oscillations were observed on $\simeq$ 6-nm particles but not on very small ($\leqslant$ 2-nm) ones. The stretching frequency of linearly bonded CO, $\simeq 2080$ cm^{-1} [this value is close to those observed [4,5] on the (111) and (100) Pt surfaces], is found to be nearly independent of the oscillation phase. The CO coverage obtained by integrating the CO IR peak area was typically lower than, or about, one half of that corresponding to saturation during CO adsorption alone. In their discussions of probable mechanisms of oscillation, FDL rule out the carbon model on the basis of earlier coking experiments [6] indicating lower CO stretching frequency in this case. The oxide model is also argued to be inapplicable because it predicts (i) higher maximum CO coverages (up to one monolayer (ML)) and (ii) a longer oscillation period (several minutes vs 35–120 s). Referring to the relatively small CO IR peak shift, FDL conclude that CO seems to be located in densely packed islands. Finally, they note that "the feedback mechanism driving the oscillations remains unclear but is most likely related to the Pt(100) or Pt(110) surface-phase transition or chlorine impurities supporting the formation of islands."

In principle, it is a reasonable idea that the oscillations under consideration are due to adsorbate-induced restructur-

* Corresponding author.
E-mail address: zhdanov@fy.chalmers.se, zhdanov@catalysis.nsk.su (V.P. Zhdanov).

0021-9517/03/$ – see front matter
doi:10.1016/S0021-9517(02)00028-3

ing of the (100) facet, or reshaping of the whole nm-sized Pt crystallites, containing primarily the (111) facets and partly the (100) facets. Experimental studies [7] of the stability of such crystallites on SiO_2 under CO- or O_2-rich conditions at temperatures typical for oscillations indicate, however, that global reshaping is unlikely on the time scale of the FDL measurements.

The situation with CO-induced surface restructuring of the (100) facets is more complex, because experimentally this process can hardly be monitored at present. Our previous Monte Carlo (MC) simulations (see Section 3.5 in Ref. [8] or Ref. [9]) show that one can construct a model predicting oscillations on this facet with facet sizes down to $\simeq 4$ nm, but whether facet restructuring on this scale is really possible or not is not clear.

Concerning oxide formation during—and as a cause of—oscillations, we note that there exist a few versions of the corresponding mean-field (MF) and MC calculations (see the review in Ref. [10]). The FDL comment that in the framework of the oxide scheme the CO coverage is expected to cycle between 0 and 1 ML is applicable only to some of the available treatments (e.g., to the MF model proposed in Ref. [11]). In contrast, the conventional MF oxide model of Sales et al. [12] easily predicts oscillations with relatively small (well below 0.5 ML) maximum CO coverage.

In our previous work [13,14], the specifics of the latter model on the nm scale were explored using the MC technique. First, we simulated [13] oscillations on lattices with sizes from 50×50 to 3×3. With decreasing size, the oscillations are found to become more irregular due to fluctuations. Sustained more or less regular oscillations may be supported for sizes down to 15×15. For smaller lattices, oscillations may easily disappear due to complete poisoning by oxygen. Our more recent study [14] was focused on such aspects as CO supply via the support and the role of this supply in synchronization of oscillations on adjacent catalyst particles. In addition, the cooperative effects in the oxide growth were treated briefly (see Figs. 12–14 in Ref. [14]). The latter effects may result in formation of oxide islands. In the simulations, segregation between oxide and CO was, however, far from perfect (the size of the oxide islands was small).

In the present study, we explore the cooperative mode of the oxide formation in more detail. In particular, besides CO diffusion, we include diffusion of adsorbed oxygen atoms into the reaction scheme. This process resulting in better phase separation was earlier neglected [14]. A deeper understanding of the problem under consideration is of interest from the point of view of the general theory of the kinetics of heterogeneous catalytic reactions (note that detailed simulations of phase separation in reactions occurring on supported catalysts are in fact lacking). In addition, the results obtained are expected to help to interpret the FDL-type experiments (see discussion in Section 4) and may also be useful for applications related to optimization of automotive catalytic converters [15]. (Due to the legislation-driven trend toward lean combustion, such converters often work in transient ignition–extinction regimes, which are close to the conditions for oscillation.)

2. Model

The first MF oxide model was proposed by Sales et al. [12] in order to interpret their observations of kinetic oscillations during CO oxidation on a Pt wire. At that time, there were no convincing experimental data supporting the connection of the oscillations with oxide formation. Later on, using low-energy electron diffraction, temperature-programmed desorption, and X-ray photoelectron spectroscopy, Vishnevskii and Savchenko [16] demonstrated that the oxide formation really plays an important role in oscillations on Pt(110), especially during long runs. More recently, Rotermund et al. [17] have also explicitly observed oxide formation during oscillations on Pt(110) on the μm scale by employing the photoelectron emission microscope. Despite these and other findings (for a review, see Ref. [17]), the understanding of the details of the oxide formation is still limited, especially on small supported particles.

In our MC simulations, following Sales et al. [12], we adopt the reaction scheme including the conventional steps of CO oxidation,

$$CO_{gas} \rightleftharpoons CO_{ads}, \tag{1}$$

$$(O_2)_{gas} \rightarrow 2O_{ads}, \tag{2}$$

$$CO_{ads} + O_{ads} \rightarrow (CO_2)_{gas}, \tag{3}$$

combined with the oxide formation and removal (reduction),

$$O_{ads} \rightarrow O^*_{ads}, \tag{4}$$

$$CO_{ads} + O^*_{ads} \rightarrow (CO_2)_{gas}, \tag{5}$$

where O^* is the oxide (or subsurface) form of oxygen (the subscripts "gas" and "ads" mark gas-phase and adsorbed particles, respectively). CO adsorption (step (1)) is assumed to occur on Pt directly and also via the shallow states above oxide. The other steps are considered to be elementary.

The kinetics predicted by the scheme above depend on the ratios between the rates of elementary reaction steps and reactant diffusion. In CO oxidation during oscillations (at $T \simeq 500$ K and reactant pressures up to a few Torr), diffusion of adsorbed CO molecules is much faster than the Langmuir–Hinshelwood (LH) step (3), which is rapid compared to reactant adsorption. The slowest processes are the substrate oxidation and reduction. Oxygen diffusion is often neglected in MC simulations of CO oxidation, because this process is much slower than CO diffusion. The rate of oxygen diffusion may be less than, comparable to, or even slightly higher than that of the LH step (see the discussion in Ref. [18]). In the latter two cases, the oxide formation may depend on oxygen mobility. For these reasons, oxygen diffusion is included in our present simulations.

The Pt catalyst particle is represented by an $L \times L$ square lattice with no-flux boundary conditions. In the bulk of the simulations, all the sites (except the boundary sites) are considered to be equivalent. Some of the runs were performed assuming the sites located in the center of the lattice to be different compared to those situated on the periphery. The latter version of the model was adopted to illustrate the interplay of (111) and (100) facets on small particles.

CO adsorption is considered to occur with the same probability on vacant sites and on sites occupied by oxide (this assumption makes sense because the initial CO sticking coefficient is often close to unity on different surfaces). The CO binding energies on these sites are considered to be appreciable (about 30 kcal/mol) and small ($\leqslant 5$ kcal/mol), respectively. In both cases, CO may diffuse and desorb. In addition, CO may jump from oxide sites to nearest-neighbour (nn) vacant sites and back. Physically, CO adsorption on the oxide sites is treated using a precursor-type scheme. Inclusion of CO precursor states above the oxide sites in the model is important because CO adsorption via such states significantly enhances oscillations in the case of the cooperative mode of oxide growth [14].

O_2 adsorbs dissociatively on pairs of nn vacant sites. Diffusion of oxygen atoms occurs via jumps to nn vacant sites. To increase the tendency of oxide growth near the oxide-island boundaries, we introduce attractive nn O–O* interaction, $\epsilon_1 < 0$. The effect of these interactions on O jumps is described using the so-called initial-state dynamics with the normalized jump probability given by [19]

$$P_{\mathrm{IS}} = \exp(\epsilon_i / k_{\mathrm{B}} T), \tag{6}$$

where ϵ_i is the O–O* interaction in the initial state (the subscript i indicates an arrangement of particles).

Reactions (3) and (5) occur between nn particles with the prescribed probabilities. The probability of step (5) is considered to be small compared to that of step (3), because the oxide is less reactive towards CO_2 formation.

In MF and MC simulations of oscillatory reaction kinetics, oxide formation has often been treated as a first-order reaction. A more common picture is that metal oxidation—i.e., conversion from chemisorbed to oxide-form oxygen—occurs via nucleation and growth of 2D oxide islands. On nm-sized particles, nucleation and growth of oxide are likely to start primarily on edges or on open facets with a small total area. To illustrate what may occur in this case, we analyse the simplest model describing this mode of oxide growth. Specifically, we assume that the lattice boundary sites play a role of nucleation centers. Oxide on the boundary sites is assumed to be more stable than on the facets and accordingly these sites are prescribed to be occupied by O* irrespective of the state of adjacent sites (practically this means that step (5) does not occur on the boundaries). Oxide is considered to grow in a cooperative manner so that the transition O $\rightarrow$ O* (step (4)) is realized with the prescribed probability only when an O atom has at least one O* neighbour. O* diffusion is neglected, because this process is assumed to be slow.

To characterize the relative rates of reaction (steps (1)–(5)) and CO diffusion, we introduce the dimensionless parameters p_{rea}. These processes are run with the probabilities p_{rea} and $1 - p_{\mathrm{rea}}$, respectively. More specifically, we use the number $N_{\mathrm{dif}} \equiv (1 - p_{\mathrm{rea}})/p_{\mathrm{rea}}$ characterizing the ratio of the rates of CO diffusion and reaction.

O diffusion is assumed to be one or two orders of magnitude faster than the catalytic cycle. In reality, CO diffusion is much faster than O diffusion. If, however, O diffusion is relatively rapid compared to reaction, the results of simulations become independent of the rate of CO diffusion provided that the latter rate is equal to or higher than that of O diffusion, because under this condition CO molecules are distributed nearly at random on the sites which are free of oxygen. In other words, there is no need to employ very high rate of CO diffusion in order to mimic reality. In our simulations, CO diffusion is considered to be two orders of magnitude faster than the catalytic cycle; i.e., we use $N_{\mathrm{dif}} = 100$.

Inside the catalytic cycle, we employ the probabilities $p_{\mathrm{ad}}^{\mathrm{CO}}$, $p_{\mathrm{ad}}^{\mathrm{O_2}}$, p_{des}, and p_{pr} for CO and O_2 adsorption, CO desorption, and CO jumps to the precursor states on the oxide sites, respectively. The rate of the LH step (3) is considered to be proportional to $1 - p_{\mathrm{des}} - p_{\mathrm{pr}}$. In addition, we introduce the parameters p_{ox} and p_{red} characterizing the rates of oxide formation and removal (steps (4) and (5)).

To describe CO molecules weakly adsorbed on the oxide sites, we use the dimensionless parameter $\mathcal{P}_{\mathrm{des}}$. The rates of CO desorption from and jumps these sites are considered to be proportional to $\mathcal{P}_{\mathrm{des}}$ and $1 - \mathcal{P}_{\mathrm{des}}$, respectively. Taking into account the detailed balance principle, we have [14] $\mathcal{P}_{\mathrm{des}} = p_{\mathrm{des}}/(p_{\mathrm{des}} + p_{\mathrm{pr}})$. This relation was employed in the simulations.

MC simulations of the steps described above are complicated by the fact that in reality the ratios of the rate constants of processes with participation of CO in the precursor and chemisorbed states extend over many orders of magnitude. In our study, we use a MC algorithm specially designed for this case. Specifically, elementary steps with participation of gas-phase chemisorbed particles are executed sequentially on sites chosen at random. If, however, a CO molecule passes to a precursor state, the calculations are switched to the elementary moves of this molecule and performed until it desorbs or makes a transition to the chemisorbed state (for the details of the algorithm, see Ref. [14]).

All the MC runs started from a clean lattice. Time was measured in MC steps (MCS). One MCS is defined as $L \times L$ attempts at adsorption–reaction events. Simulating these events, we consider that the sum of the probabilities of CO desorption, CO jumps to the precursor states, and LH reaction equals unity. This means that the MC and real times are interconnected as $t_{\mathrm{MC}} = (k_{\mathrm{des}} + k_{\mathrm{pr}} + k_{\mathrm{LH}})t$, where k_{des}, k_{pr}, and k_{LH} are the rate constants for the steps mentioned above.

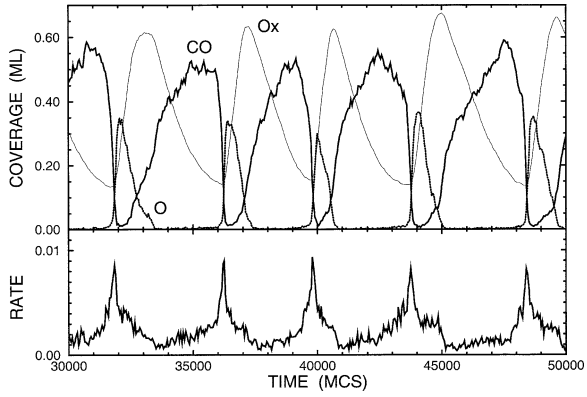

Fig. 1. CO, O, and O^* (Ox) coverages and reaction rate (CO_2 molecules per site per MCS) as a function of time for $p_{ad}^{CO} = 0.0095$. The other parameters are standard: $p_{ad}^{CO} + p_{ad}^{O_2} = 0.02$, $p_{des} = 0.002$, $p_{pr} = 0.02$, $p_{ox} = 0.005$, $p_{red} = 0.004$, $\epsilon_1/k_BT = -2$, $N_{dif} = 100$, and $L = 50$. Oxygen diffusion is one order of magnitude faster than the catalytic cycle.

3. Results of simulations

Typical parameters used in simulations were $p_{ad}^{CO} + p_{ad}^{O_2} = 0.02$, $p_{des} = 0.002$, $p_{pr} = 0.02$ (with these values of p_{des} and p_{pr}, we have $\mathcal{P}_{des} \simeq 0.1$), $p_{ox} = 0.005$, $p_{red} = 0.004$, $\epsilon_1/k_BT = -2$, $N_{dif} = 100$, and $L = 50$. p_{ad}^{CO} was a governing parameter.

With the parameters above, well-developed oscillations are observed at $p_{ad}^{CO} \simeq 0.0095$. Examples of oscillatory kinetics and lattice snapshots, obtained in the case when oxygen diffusion is one order of magnitude faster than the catalytic cycle, are shown in Figs. 1 and 2.

With decreasing p_{red} from 0.004 down to 0.002, the oscillation period becomes about two times longer (cf. Figs. 1 and 2 with 3 and 4).

With increasing rate of oxygen diffusion by one order of magnitude (Figs. 5 and 6), the size of the oxide islands

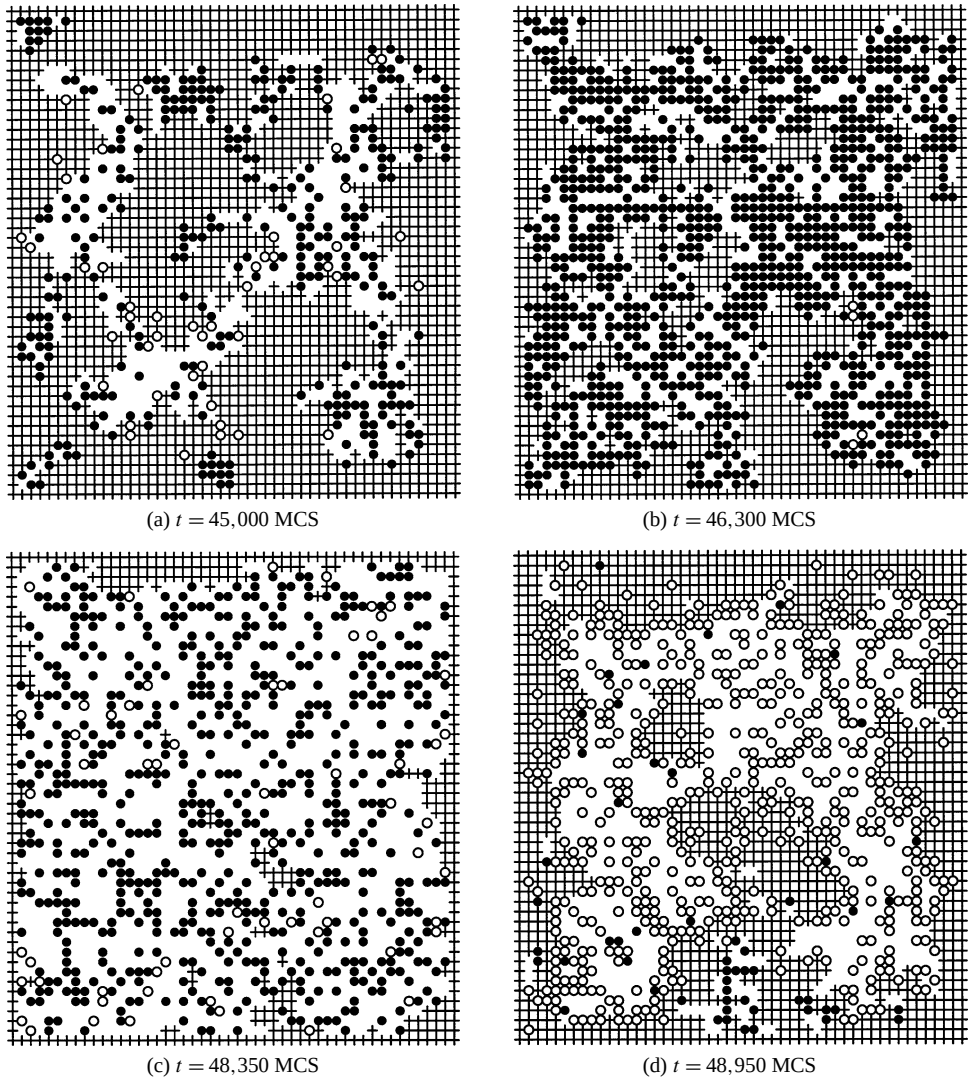

(a) $t = 45{,}000$ MCS (b) $t = 46{,}300$ MCS

(c) $t = 48{,}350$ MCS (d) $t = 48{,}950$ MCS

Fig. 2. Snapshots of the lattice for the MC run, shown in Fig. 1, in the cases when the oxide coverage is (a) maximum, (b) between maximum and minimum, (c) minimum, and (d) between minimum and maximum. Filled circles, open circles, and plus signs correspond to CO, O, and O^*, respectively. Vacant sites are not indicated.

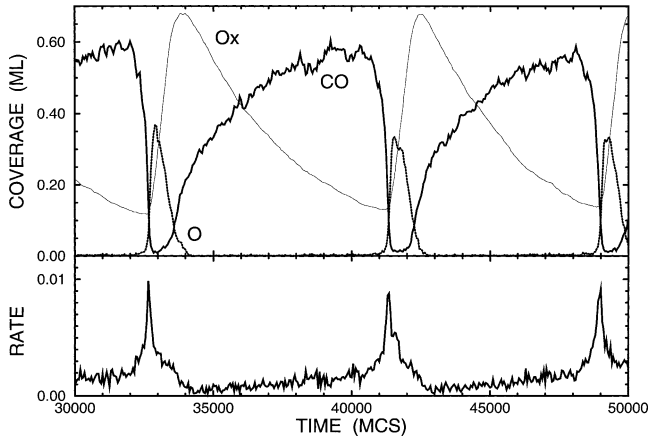

Fig. 3. As Fig. 1 for $p_{red} = 0.002$.

increases slightly (cf. Figs. 2b and 6b). The oscillation period increases as well (cf. Figs. 1 and 5). If in addition the lattice size is reduced from 50 to 30 (Figs. 7 and 8), the role of the boundary oxide sites becomes more important. For this reason, the oxide coverage slightly increases (cf. Figs. 5 and 7), the maximum CO coverage decreases, and the oscillation period becomes somewhat longer.

To illustrate the interplay of different facets, we used a (50×50) lattice with the boundary sites and the central (26×26) array of sites occupied by O^* irrespective of the state of adjacent sites. This model mimics the case when the Pt particle is shaped into a truncated pyramid with a top (100) facet, and (111) side facets and with the largest (100) facet attached to the support. Oxide on the (100) facet is expected to be more stable than on the (111) facets. To show what may happen in this case, the oxide on the boundary

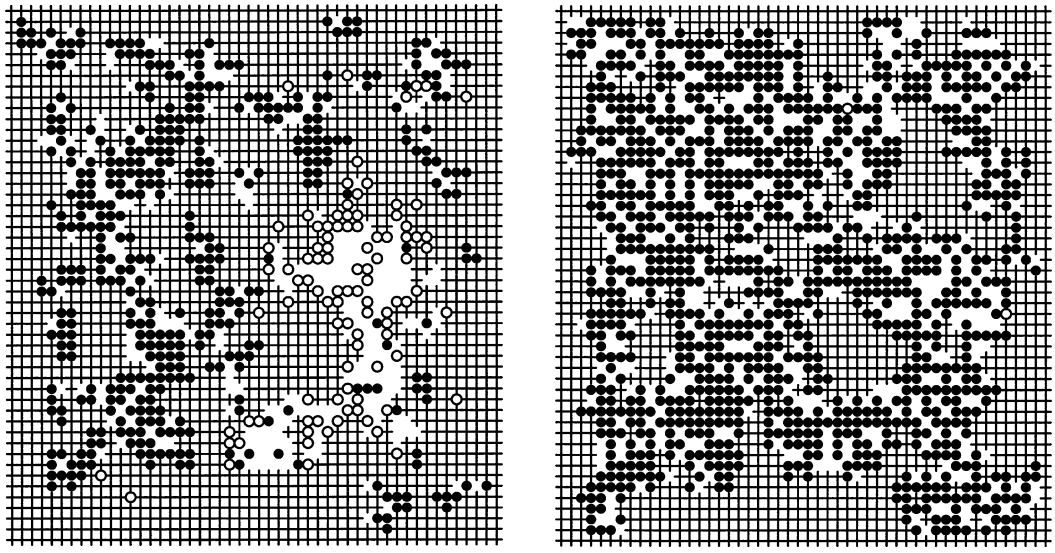

(a) $t = 33{,}800$ MCS (b) $t = 36{,}200$ MCS

(c) $t = 41{,}100$ MCS (d) $t = 41{,}190$ MCS

Fig. 4. Lattice snapshots for the MC run, presented in Fig. 3. The designations are as in Fig. 2.

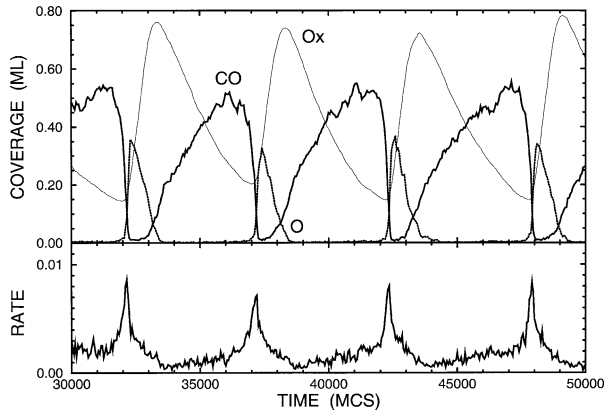

Fig. 5. As Fig. 1 for the case when oxygen diffusion is two orders of magnitude faster than the catalytic cycle.

sites and on the top facet, represented by the central array of sites, is assumed to be less reactive towards CO. It facilitates the formation of oxide on the (111) facets (the peripheral part of the lattice) but cannot be removed via step (5). With these assumptions, the model predicts much higher average oxide coverage and accordingly much lower maximum CO coverage (cf. Figs. 1 and 9). The lattice snapshots (Fig. 10) corresponding to this case are of course quite different from to those obtained for the uniform lattice (Figs. 2, 4, 6, and 8).

4. Discussion

Our earlier MC simulations [13] show that in the framework of the oxide model one can obtain more or less regular oscillations for sizes down to 15×15. Practically, this means

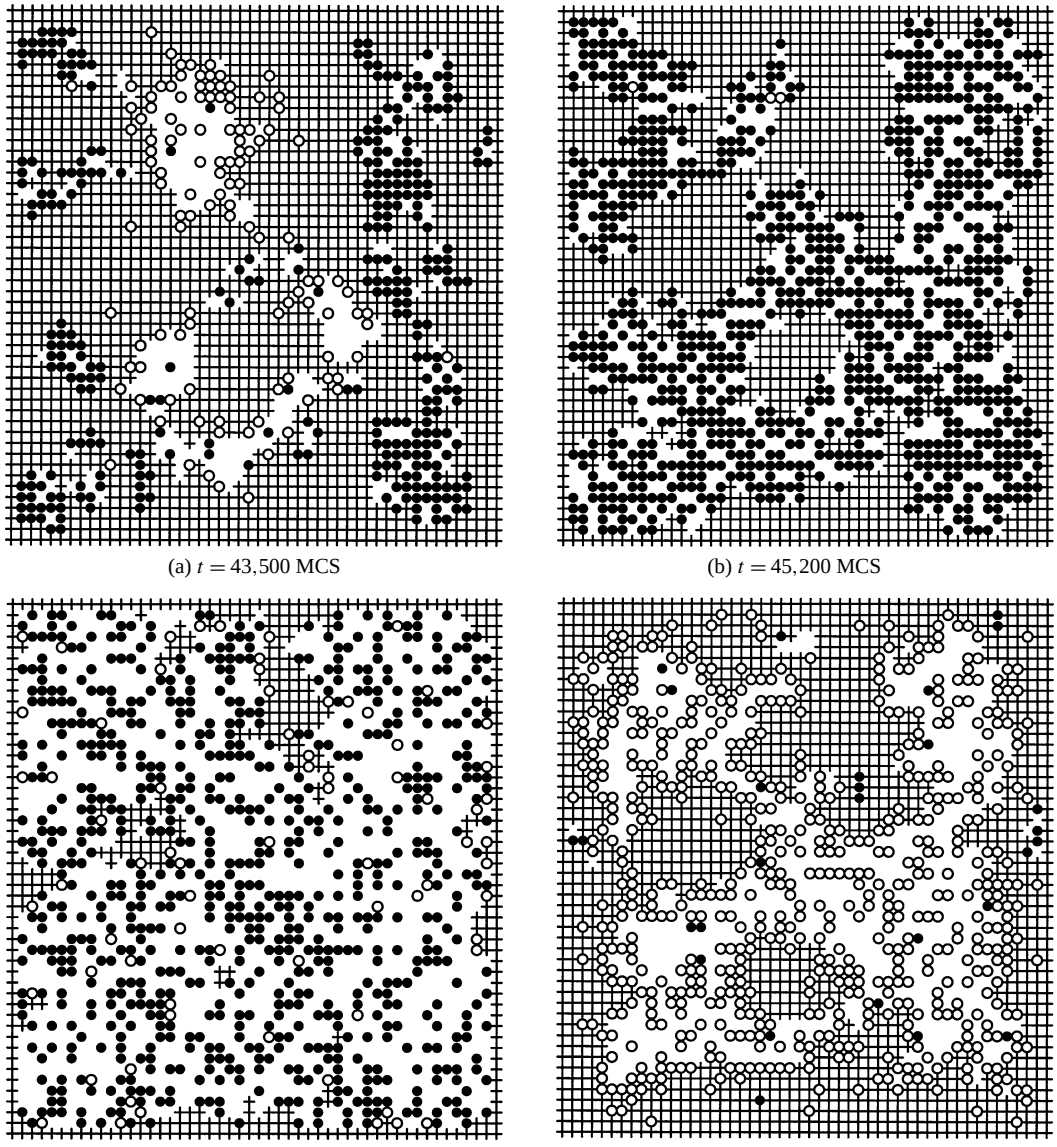

(a) $t = 43{,}500$ MCS (b) $t = 45{,}200$ MCS

(c) $t = 47{,}800$ MCS (d) $t = 48{,}400$ MCS

Fig. 6. Lattice snapshots for the MC run, shown in Fig. 5. The designations are as in Fig. 2.

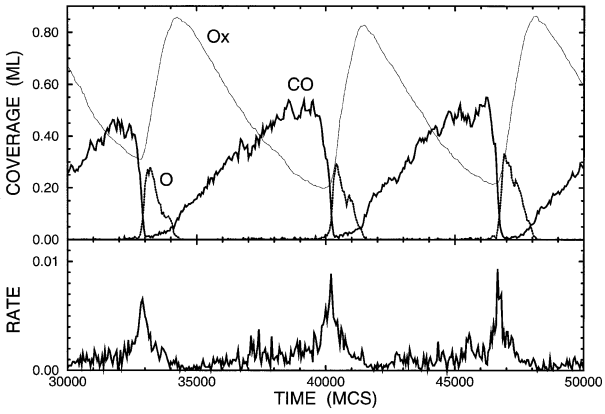

Fig. 7. As Fig. 5 for $L = 30$.

that oscillations are possible for Pt particles with diameters above $\simeq 4$ nm. This finding is in agreement with experiments [3] indicating that the critical particle size for oscillations is about 4 nm. Synchronization of such oscillations is expected to occur via the gas phase. (Some of the particles, e.g., those with sizes much below the average size, may of course fail to meet the conditions for synchronization.)

In our present simulations, we have illustrated that during kinetic oscillations resulting from the oxide formation the maximum CO coverage may be appreciably smaller than 1 ML (see, e.g., Figs. 7 and 9) and segregation between oxide and CO may be remarkable (see, e.g., Figs. 6a and 6b or 10b). The latter means that the shift of the stretching frequency of CO may be nearly negligible. Thus,

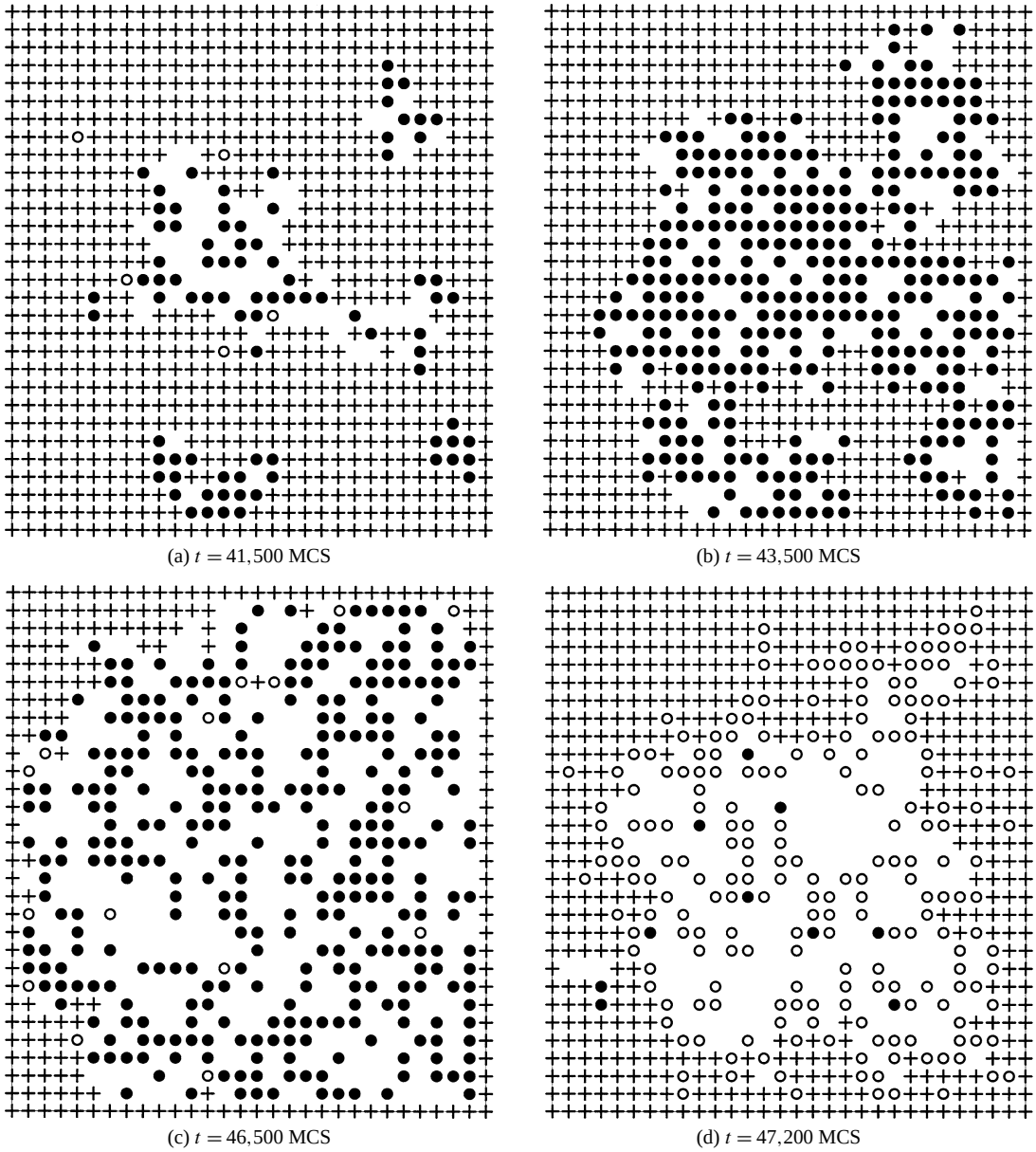

(a) $t = 41{,}500$ MCS (b) $t = 43{,}500$ MCS

(c) $t = 46{,}500$ MCS (d) $t = 47{,}200$ MCS

Fig. 8. Lattice snapshots for the MC run, exhibited in Fig. 7. The designations are as in Fig. 2.

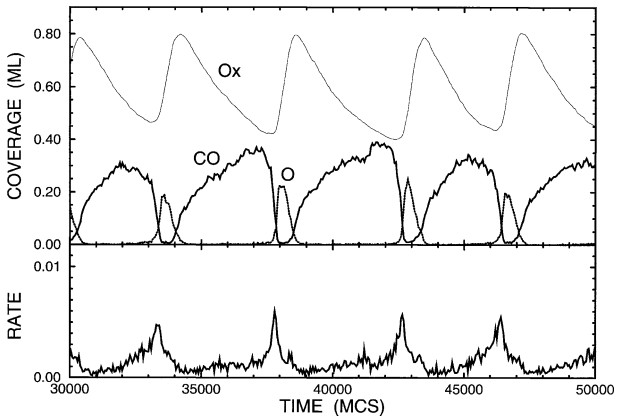

Fig. 9. CO, O, and O^* (Ox) coverages and reaction rate (CO_2 molecules per site per MCS) as a function of time for the case when, in addition to the boundary sites, the central (26×26) part of the (50×50) lattice is occupied by O^* irrespective of the state of adjacent sites. The parameters are as in Fig. 5 except that $p_{ad}^{CO} = 0.009$.

the two main arguments of FDL [3] against the oxide model (see Section 1) do not seem to hold. The third argument, concerning the fact that the oxide model predicts a longer oscillation period (several minutes vs 35–120 s, respectively) might be right if the oxide growth were described by a simple first-order equation. This is, however, not the case. Physically, it is clear that the time scale of the oxide formation depends on the size of the oxide islands. On nm-sized Pt particles, the island size is expected to be smaller than that on the single- or polycrystal samples and accordingly the corresponding time scale may be shorter or even much shorter.

5. Conclusion

In summary, our MC simulations demonstrate that one can construct an oxide model exhibiting phase separation

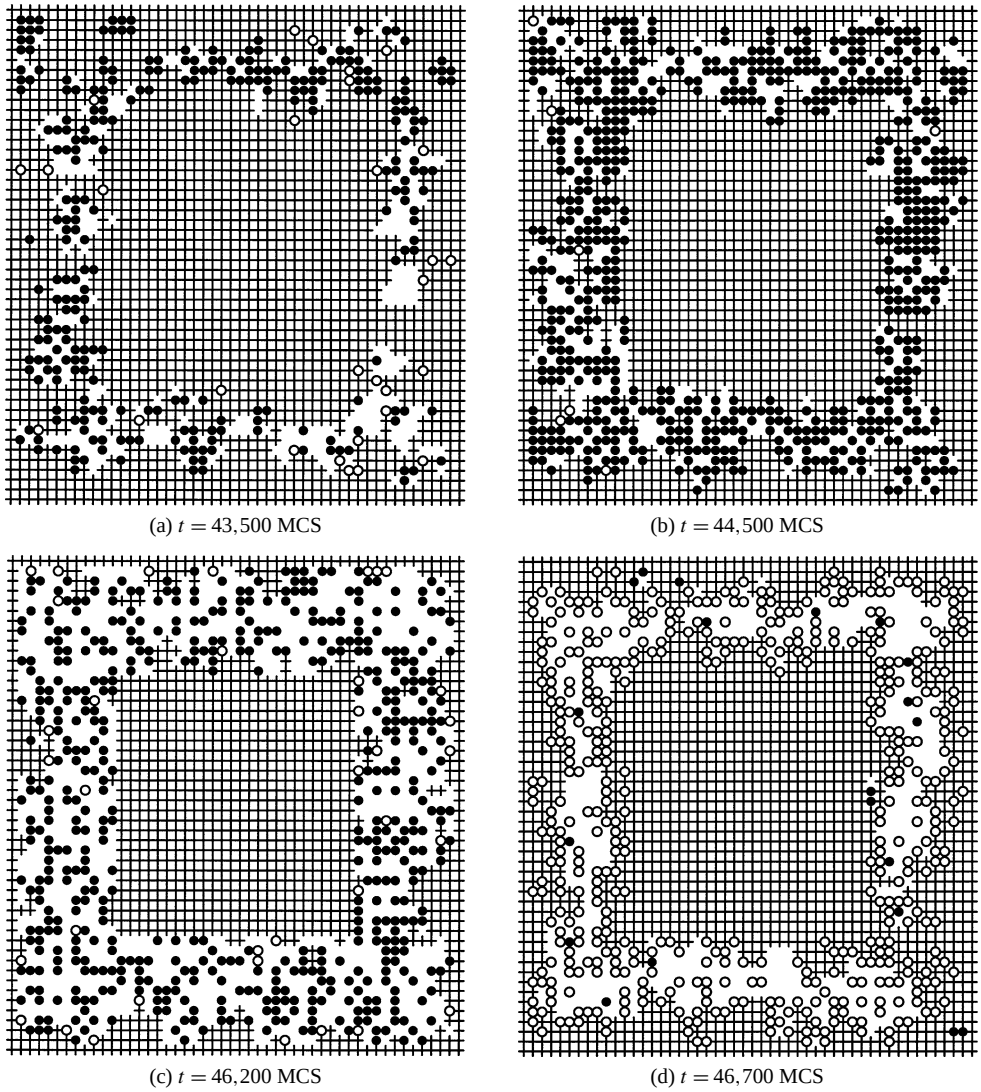

(a) $t = 43{,}500$ MCS (b) $t = 44{,}500$ MCS

(c) $t = 46{,}200$ MCS (d) $t = 46{,}700$ MCS

Fig. 10. Lattice snapshots for the MC run, shown in Fig. 9. The designations are as in Fig. 2.

on the nm scale and oscillatory kinetic behaviour similar to those observed [3] in CO oxidation on supported Pt. Thus, one cannot rule out oscillations in this system being related to oxide formation. Moreover, we believe that the oxide mechanism is actually the most probable because recent experimental data [17], obtained on single-crystal Pt surfaces, indicate that oxide formation often plays a more important role in oscillations than one could expect earlier.

Finally, it is appropriate to repeat that at present the experimental data on the details of the surface oxide formation on Pt are still scarce (new opportunities here are related to the use of model supported catalysts [20,21]). For this reason, we tried to keep our model as simple as possible. Some presumably reasonable elements of the complexity were introduced only to the part related to the oxide growth in order to illustrate the possibility of segregation between oxide and CO. Many other details might easily be introduced into the model as well. For our present goals, it was, however, not necessary. With the ingredients we incorporated, our study shows that the MC technique may effectively be used to analyse many interesting aspects of the nm chemistry which are beyond the conventional MF approximation.

Acknowledgments

This work was supported by the Competence Center for Catalysis at Chalmers University of Technology (Grant 4F7-97-10929), which is financed by the Swedish National Energy Administration and member companies including AB Volvo, Johnson Matthey-CSD, Saab Automobile AB, Perstorp AB, MTC AB, Eka Chemicals, and the Swedish Space Corporation.

References

[1] P. Hugo, Ber. Bunsenges. Phys. Chem. 74 (1970) 121.
[2] F. Schüth, B.E. Henry, L.D. Schmidt, Adv. Catal. 39 (1993) 51.
[3] P.T. Fanson, W.N. Delgass, J. Lauterbach, J. Catal. 204 (2001) 35.
[4] R.G. Tobin, P.L. Richards, Surf. Sci. 179 (1987) 387.
[5] R. Martin, P. Gardner, A.M. Bradshaw, Surf. Sci. 342 (1995) 69.
[6] J.A. Anderson, F.K. Chong, C.H. Rochester, J. Mol. Catal. A Chem. 140 (1999) 65.
[7] L. Österlund, B. Kasemo, to be published.
[8] V.P. Zhdanov, B. Kasemo, Surf. Sci. Rep. 39 (2000) 25.
[9] V.P. Zhdanov, B. Kasemo, Surf. Sci. 513 (2002) L385.
[10] V.P. Zhdanov, Surf. Sci. Rep. 45 (2002) 231.
[11] M.R. Bassett, R. Imbihl, J. Chem. Phys. 93 (1990) 811.
[12] B.C. Sales, J.E. Turner, M.B. Maple, Surf. Sci. 114 (1982) 381.
[13] V.P. Zhdanov, Catal. Lett. 69 (2000) 21.
[14] V.P. Zhdanov, B. Kasemo, Surf. Sci. 511 (2002) 23.
[15] P.-A. Carlsson, M. Skoglundh, E. Fridell, E. Jobson, B. Andersson, Catal. Today (2002), in press.
[16] A.L. Vishnevskii, V.I. Savchenko, Kinet. Catal. 31 (1990) 99.
[17] H.H. Rotermund, M. Pollmann, I.G. Kevrekidis, Chaos 12 (2002) 157.
[18] V.P. Zhdanov, B. Kasemo, Surf. Sci. 412 (1998) 527.
[19] F. Nieto, A.A. Tarasenko, C. Uebing, Def. Diffus. Forum 162 (1998) 59.
[20] C.R. Henry, Surf. Sci. Rep. 31 (1998) 23.
[21] J. Libuda, H.-J. Freund, J. Phys. Chem. B 106 (2002) 4901.